INDUCING MECHANICAL STRESSES IN ELECTROACTIVE HYDROGELS TO INFLUENCE THE FATE OF MESENCHYMAL STEM CELLS

By

KRITI GUPTA

A thesis submitted to the

School of Graduate Studies

Rutgers, The State University of New Jersey

In partial fulfillment of the requirements

For the degree of

Master of Science

Graduate Program in Biomedical Engineering

Written under the direction of

Ronke Olabisi

And approved by

_____

_____

_____

New Brunswick, New Jersey

October, 2018

ABSTRACT OF THE THESIS

Inducing Mechanical Stresses in Electroactive Hydrogels to Influence the Fate of Mesenchymal Stem Cells

by KRITI GUPTA

Thesis Advisor:

Ronke Olabisi

Mesenchymal stem cells (MSCs) can differentiate into bone, cartilage, muscle, tendon, and other mesenchyme-derived tissue with the right treatment of growth factors or the right mechanical stimuli. Therefore, these cells are widely used in tissue engineering. Though the MSC response to biochemical signals is well understood, their response to biophysical signals is still being described. Exploring the behavior of MSCs in response to a variety of biochemical, biophysical, or bioelectrical signals can lead to better scaffolds for tissue engineering. Scaffolds do not entirely mimic the native environment that cells experience, particularly for excitable tissues. For instance, in their native environment smooth muscle cells experience contraction and relaxation. While electroactive materials can deform, at present, few such materials are suitable as cell scaffolds. Herein, this thesis describes the development of poly(ethyelene glycol) diacrylate – poly(acrylic acid) (PEGDA-PAA) as an electroactive scaffold for MSCs. PEGDA-PAA hydrogels experience a change in volume with the application of an electric field, producing bending, wave-like movements similar to that of smooth muscle. Electroactive hydrogels were capable of deformation and

seeded cells proliferated on the surface. Ongoing work is investigating a stimulation profile for the hydrogels that will be nonlethal for cells.

ACKNOWLEDGEMENTS

I would like to thank Dr. Olabisi for all her patience and guidance in the past 4 years. Thank you for giving me the opportunity to conduct research and apply what I learned in my classes. That experience was one of the most valuable in my time in undergrad and graduate school.

Thank you Dr. Berthiaume and Dr. Freeman for your mentorship in multiple facets of my educational career. Dr. Berthiaume, it was a pleasure to have you as a professor in one of my first years of college, as my senior design mentor and finally as my thesis advisor. Thank you Dr. Freeman for allowing me to receive guidance from individuals in your lab and your laboratory resources that were imperative for my experiments.

Finally I would not be where I am today with the unconditional support of my family and friends. Mom and Dad, there is not enough I can say for everything you have done for me. Thank you for always being there. Yukti, thanks for always having an ear for anything I need to talk about. Kai you have been a support beam day in and day out – thank you for walking beside me and your patience and understanding through everything. And my closest friends for being only a message or call away when life gets hard and agreeing to go on wild adventures with me– thank you.

TABLE OF CONTENTS

LIST OF FIGURES

LIST OF ABBREVIATIONS

α-MEM	Alpha-Minimum Essential Media
AA	Acrylic Acid
ACE	2,2-Dimethoxy-2phenylacetophenone
ACRL	Acryloyl
GTA	Glutaraldehyde
ECM	Extracelluar Matrix
HBS	HEPES Buffered Saline
NVP	1-vinyl-2-pyrrolidinone
MSCs	Mesenchymal Stem Cells
PAA	Poly(acrylic acid)
PBS	Phosphate Buffered Saline
PCL	Polycaprolactone
PEGDA	Poly(ethylene glycol) diacrylate
PEGDA-PAA	Poly(ethylene glycol) diacrylate – Poly(acrylic acid)
SVA	Succinimidyl valerate
UV	Ultraviolet

CHAPTER 1. Introduction

Tissue engineering is a field in bioengineering that incorporates the use of cells, scaffolds, and external stimuli to develop biological substitutes for tissue repair and regeneration. Stem cells are widely used in tissue engineering therapies because they can differentiate into numerous tissue types. For instance, mesenchymal stem cells (MSCs) have been embedded into scaffolds to form tissue-like constructs that promote bone formation. [1] They have been incorporated into decellularized extracellular matrices that have served as scaffolds for repairing injured menisci. [2] Bone marrow-derived MSCs have the ability to differentiate into neuronal cell types for further use in neural disease therapy. [3, 4] MSCs used to develop these tissues are dependent on the scaffolds supporting them. Mechanical influences from scaffolds can significantly impact tissue morphogenesis. [5-7] For instance, when seeded on scaffolds with elastic moduli that resemble bone, muscle, or brain tissue, MSCs have been shown to differentiate into osteoblasts, myoblasts, or neurons. [8-11] External loading on the scaffolds is also important—studies show that compressive forces induce signaling pathways that promote chondrogenesis while tension promotes osteogenesis. [8, 12, 13]

Understanding the effects of biophysical cues on MSCs can lead to better scaffolds for tissue engineering. A primary challenge in the field is building scaffolds that better mimic the native environment that cells experience. For cells from excitable tissues, one proposed solution is the use of electroactive scaffolds. Electroactive scaffolds are 3D biocompatible structures that contain ionic bonds that are responsive to electrical stimulation. These scaffolds, specifically hydrogels, can harness electrical impulses to power mechanical movement in ionic aqueous solutions. In addition to their potential as scaffolds for

excitable tissues, these polymers could be designed to deliver mechanical loads to cells in a compact, tissue culture-friendly manner. Current studies that expose MSCs to cyclic strain do so with the use of large, heavy, complicated pieces of equipment. [14, 15] Burk et al. used a custom-made bioreactor to apply cyclic strain to MSCs seeded on a decellularized tendon matrix that resulted in cell alignment and altered expression indicating tendon-related genes. [16] When the scaffolds were exposed to longer durations of mechanical stimuli, cell viability decreased whereas short stimulation periods enhanced effects such as increased proliferation due to mechanical stimulation. Since custom-made devices do not lend themselves to reproducibility across research groups, to further understand cell behavior in response to mechanical loading, simpler, more reproducible methods to probe cell response are required. Electroactive scaffolds are a viable alternative because they can deform with short bursts of electrical stimulation and produce similar strain that cells in excitable tissues would experience *in vivo* via a simple, reproducible scaffold.

CHAPTER 2. Background

2.1 Tissue Engineering

Tissue engineering is the targeted combination of cells, scaffolds, and biochemical signals to grow new tissues and organs. The goal of the new tissues and organs would be to replace or repair damaged tissues, ultimately eliminating the need for organ donation.

2.1.1 Mesenchymal Stem Cells

MSCs are one of the key contributors in tissue engineering especially in the tissue regeneration and repair space. Researchers aim to understand and guide the behavior of stem cells to grow and repair targeted tissues. MSCs are well characterized and readily available in adult bone marrow and fat. Their multipotency allows them to have a diverse differentiation profile that includes chondroctyes, osteocytes, myocytes, and adipocytes, among others. They do not carry the ethical concerns of embryonic stem cells and they are highly proliferative *in vitro*. Additionally, MSCs have greater immunosuppressive properties than induced pluripotent or embryonic stem cells. [17, 18] MSC differentiation can be mediated with chemical, biophysical, and environmental cues. [19-21] While there has been considerable work towards understanding the influence of soluble factors on MSC fate, there is also a large body of research supporting the importance of mechanical signals in influencing MSC lineage, particularly for tissue regeneration applications. [22-24] Physical signals, such as tensile and compressive loads, play a major role in constructing the *in vivo* niche for MSCs which drives their differentiation. [25] It is paramount to maintain an MSC niche when conducting *in vitro* experiments because MSCs undergo

changes that affect their differentiation and proliferation after multiple passages. [26, 27] Often these passages occur on tissue culture plastic that exposes cells to a stiff tissue environment that can alter cell behavior. [28] Researchers have shown that 3D MSC cultures show more promise for regenerative purposes than MSCs grown in 2D cultures. [29] Therefore it is important to construct a physiologically relevant environment that keeps the stemness of MSCs intact and can be designed to influence MSC fate. Biomaterial scaffolds are a modifiable, 3D landscape that can assist in delivering mechanical cues and mimicking *in vivo* surroundings for cells. Thus, these scaffolds are another significant area of focus in tissue engineering.

2.1.2 Inert Scaffolds

Biomaterial scaffolds are common substrates that can serve as tissue or extracellular matrix substitutes *in vivo* or *in vitro*. Scaffolds can be designed from sources derived from nature or synthetic materials. Natural scaffolds already contain binding sites for cells as well as other growth and signaling molecules that induce tissue remodeling. Common naturally derived components used in scaffolds include collagen, decellularized tissue, and glycosaminoglycans such as hyaluronic acid and chitosan. [30] El-Jawhari et al. showed that collagen-containing scaffolds enhanced proliferation and attachment of MSCs over non-collagen containing scaffolds. [31] Intini et al. fabricated chitosan scaffolds that showed improved wound healing in diabetic rats. [32] Composite scaffolds constructed with hydroxyapatite and alginate promoted matrix deposition and bone regeneration. [33] Naturally-derived scaffolds have also been used with MSCs. McAndrews et al. developed glutaraldehyde (GTA) scaffolds that were seeded with MSCs. They observed that

concentrations of GTA in the scaffold correlated with the amount of osteogenic differentiation. [34] Yang et al. developed a scaffold from decellularized ECM and seeded it with bone marrow-derived MSCs—the scaffolds were implanted into mice and cartilage-like tissue began to form 4 weeks later. [35] In scaffolds that use a natural material, there is often an additional step that requires the material to be processed, such as undergoing decellularization, to meet initial material standards and ensure reproducibility. This process can leave behind toxins such as detergents that result in varying degrees of immunogenicity. [36] Furthermore, their remaining intrinsic cues confound observations describing how mechanical properties affect cell behavior. Synthetically-derived scaffolds serve as a clean slate upon which to construct and control chemical and mechanical properties to study certain cell behavior, are highly reproducible, and their building blocks are more readily available than natural biomaterials. Synthetic scaffolds can be comprised of biocompatible polymers such as poly(ethylene glycol) diacrylate (PEGDA), poly(lactic acid), poly(glycolic acid), poly(lactic-*co*-glycolic acid) and polycaprolactone. [37, 38] Synthetic, polymeric scaffolds seeded with autologous cells to provide patients with artificial heart valves showed reduced immunogenicity compared to the current gold standards which include either mechanical valves or xenografts. [39] Zhuravleva et al. assessed electrospun polyamide-6 based scaffolds seeded with MSCs and showed that the cells adhered and exhibited some proliferation and elongation. Additionally, these scaffolds supported a greater mechanical load than native ECM. [40] After MSCs were seeded on scaffolds developed with poly(ε-caprolactone), researchers observed chondrogenic gene expression and histology. [41] Despite these successes, scaffolds for excitable tissues do not respond to external stimuli in the manner that the native tissues do.

2.1.3 Mechanotransduction

There are extensive studies in which researchers use apparatuses that stretch scaffolds to mechanically stimulate them with strain. Haghighipour et al. exposed MSCs to 10% cyclic uniaxial strain that resulted in their differentiation into skeletal muscle cells. [42] Ghanzafari et al. designed a custom device to deliver a 0-25% range of tensile strain that caused the proliferation and differentiation of MSCs into smooth muscle cells. [14] Leong et al. exposed human MSCs (hMSCs) to cyclic tensile loads for 8 hours, which resulted in the upregulation of neurogenic genes. [43] Song et al. used a cell stretching device (Model ST-140, STREX Co., Ltd, Osaka, Japan) for 24-48 hours at 10% strain on rat bone marrow MSCs that resulted in cell morphology changes towards tendon and ligaments formation. [15] Although successful in their applications, these devices have their limitations. They cannot be used *in vivo* and have scaffold size requirements. Furthermore, excitable tissues provide cells a particularly dynamic environment that stretching devices may not be able to mimic. Scaffolds that do not require cell stretching devices to undergo strain may be more suited to replicating excitable tissues. [44]

2.2 Excitable Tissues

Excitable tissues respond to endogenous electrical stimulation and contractile movement. Excitable cells have membranes that contain voltage-gated ion channels and pumps to preserve a negative resting potential and respond to action potentials triggered by external stimuli (Figure 2.1). The three major types of excitable cells are muscular, cardiac, and

neural. Cells in excitable tissues contain an electric potential across their cell membrane which has allowed them to develop electrical properties. [45] For example, cardiac cells control heart rate and strength of contractions with the help of bioelectrical impulses. Cardiac tissue engineering studies have shown that delivering electrical signals *in vivo* to implanted scaffolds seeded with myocytes showed progressive development of contractile characteristics in the implanted myocytes. [46-48] Muscle fibers contract and expand under electrical control. Skeletal muscle tissue maturation is dependent on electrical impulse stimulation of myocytes via motor neurons. [49, 50] Several studies have utilized *in vitro* electrical stimulation as well. Chi et al. developed protein-carbon nanotubule scaffolds, which they seeded with fibroblasts and exposed to electrical stimulation. Fibroblasts seeded on scaffolds rendered electro-conductive with the inclusion of the carbon nanotubules had boosted collagen production compared to fibroblasts seeded on pure protein scaffolds. [51] Electrical stimulation of scaffolds with seeded neurons has enhanced nerve regeneration. [52] Electrical exposure also increased cell migration and repair in scaffolds seeded with outer and inner meniscus cells. [53] Such electro-conductive scaffolds have been well explored for their impact on cells, conversely, electroactive materials as cell scaffolds have few investigations. The motive of this thesis is to explore that knowledge gap.

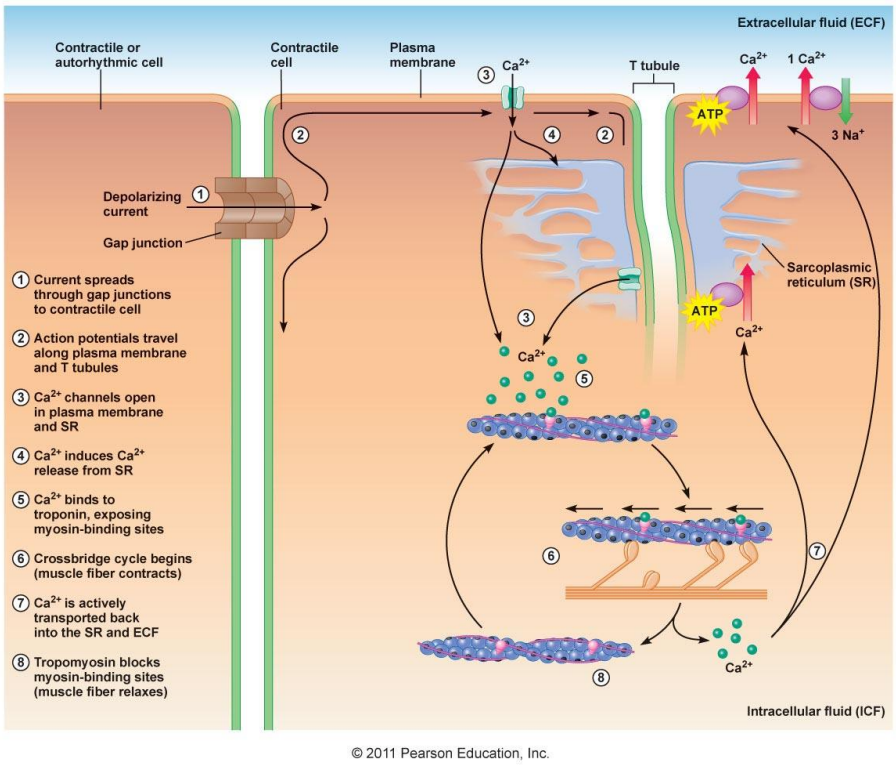

Figure 2.1 Action potential in muscle cells. An action potential triggers calcium ion channels to open, which initiates a positive feedback loop causing further release of calcium ions from the sarcoplasmic reticulum. The calcium ions bind to troponin, which reveals myosin-binding sites that permit the binding of myosin to actin, which leads muscle fiber contraction. [54]

2.3 Electroactive Materials

Electroactive materials can convert electrical stimulation to other forms of energy such as mechanical energy in the form of vibrations or deformations. They differ from electro-conductive materials in that electro-conductive materials are capable of conducting an electric current but do not change shape or volume in doing so. .

2.3.1 Types

Electroactive materials include metals, inorganic electroactive substances, metal and organic composites, and organic electroactive polymers [55, 56] Of all electroactive materials, electroactive polymers are the most widely implemented in tissue engineering applications. They are desirable because of the similarity of their physical properties to biological tissues and their capacity to induce considerable actuation strain. [57] Additionally, they have the ability to produce stresses (180 and 450 MN/m^2) 1000 times greater than the same volume of physiological muscle, can be easily fabricated, and can function in body fluids. [58, 59] They have been used as actuators, sensors, and artificial muscles. [60-64] There are two types of electroactive polymers: dielectric and ionic. Dielectric electroactive polymers are actuated by electrostatic forces between two electrodes that are directly applied – these often require large voltages. [65] Ionic electroactive polymers undergo actuation with the movement of ions within the polymer when exposed to electric fields. They require a solvent to be stimulated but not a large voltage source. Ionic electroactive polymers are most widely used in biomimetic applications such as soft robotics and cell scaffolds.

2.3.2 For Use as Soft Robotics

Soft tissue robotics using electroactive polymers has gained traction due to the ability of electroactive polymers to induce large amounts of strain in a small area. For instance, one of the drawbacks to traditional robotic prosthetic limbs is that they end up being heavier than the human version of the limb. [66] Researchers have tried to overcome this shortcoming by using electroactive polymers to build artificial muscle actuators such as

robotic fingers. [67-69] They result in more lightweight devices without increased complexity. Electroactive polymers have also been incorporated in miniature soft robots, termed “aquabots,” that mimic natural movement of aqueous life forms. Kwon et al. replicated movements of octopus-like and sperm-like aquabots with the application of alternating negative and positive voltages (Figure 2.1). [70]

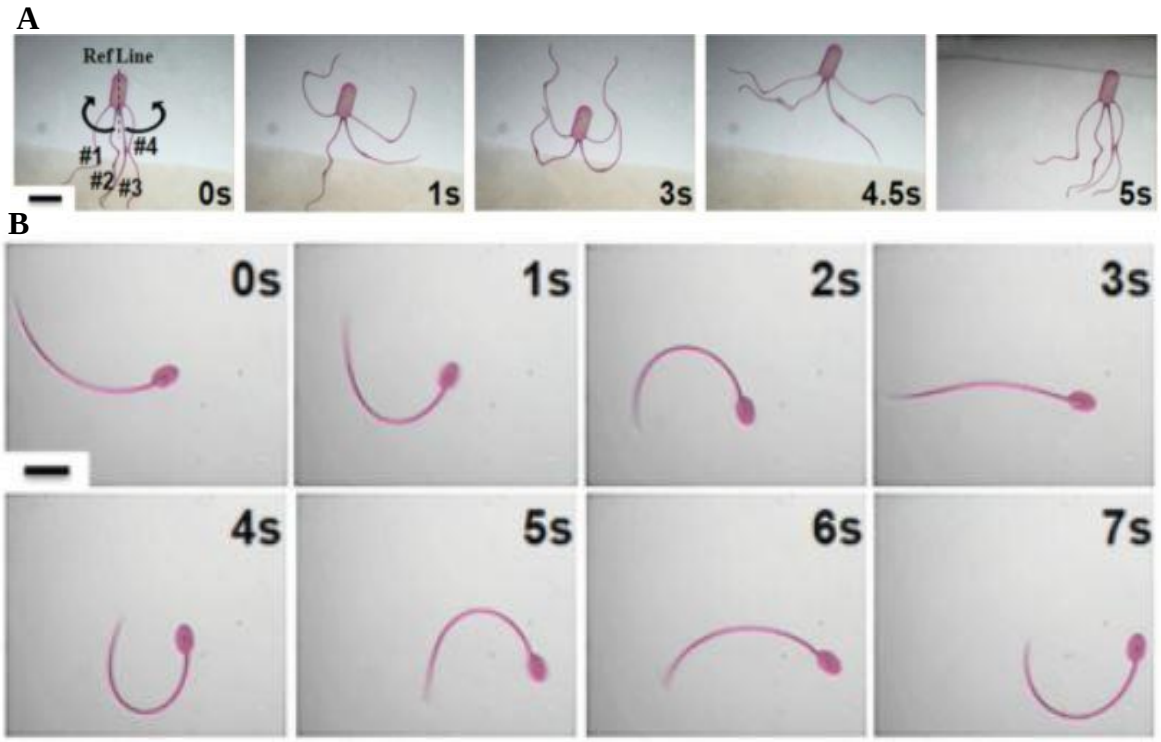

Figure 2.2 Timecourse images of an octopus aquabot (A) and a sperm aquabot (B) moving with electrical stimulation (alternating positive and negative voltage). [70]

These aquabots have the potential to be implemented in transport, capture and release, signaling, and drug delivery systems. Soft robotics can potentially be utilized in several other biomedical applications that require very small but easily guidable actuators such as microsurgical instruments, micro-catheters, and endoscopes that can be guided up the

spinal cord to access the brain or the interior of blood vessels. [59] Micro-actuators even have the potential to perform single cell manipulations by operating as optical tweezers. Jager et al. demonstrated clasping and positioning of 100 µm objects with a microrobotic arm formulated with conjugated polypyrrole. [71] Overall electroactive materials have the ability to optimize small scale robotics to improve and broaden their function but have yet to be explored as tissue engineering constructs that can support cells.

2.3.3 For Use as Cell Scaffolds

Electroactive cell scaffolds harness electrical energy and are typically made with synthetic or natural polymers. [72-75] The electrical source of stimulation can be powered from the body's natural electrical impulses or transdermally with microelectrodes at the surface of the skin for example. [76, 77] Electro-conductive scaffolds are more investigated than electroactive scaffolds. There are previous investigations of cell-seeded scaffolds that have conductive properties, which serve as a mode of electrical delivery to cells to enhance their growth and differentiation towards a certain lineage. [78-80] Mawad et al. formulated a hydrogel with a conducting polymer that was capable of supporting the proliferation of fibroblasts and myoblasts. [78] Electrical stimulation has been shown to benefit viability and increase proliferation of several cell types such as neural cells, cardiac muscle cells, bone cells and fibroblasts and epithelial cells for wound healing. [74, 81-86] However, there are few reports of how these cells behave on electroactive scaffolds. One of the attractive benefits of electroactive scaffolds is their ability to react to external stimuli after synthesis by deforming. There have been several studies that induce bending in electroactive hydrogels towards the goal of developing tissues e.g., artificial muscles, but

actuation conditions have been too harsh for cellular environments. Li et al. developed polyelectrolyte hydrogels and varied the electric field strength exposed to the hydrogels as well as the aqueous solution, sodium sulfate, used to immerse the hydrogels in. The degree of bending was greatest at the highest electric field strength, 357 V/m and at 0.05 M of sodium sulfate. [87] However, this high voltage and the saline solution are both lethal to cells. Kwon et al. developed a polymer hydrogel that exhibited bending when exposed to different voltages ranging from 1.5 to 6.5 volts. [88] The saline solution (0.002 M NaCl) used to actuate the hydrogels was more suitable for supporting cells. However, no cell studies were performed on these hydrogels. Thus it is impossible to know whether the hydrogel material itself was cytotoxic. A number of investigations demonstrate successful actuation of electroactive hydrogels, but all contain similar limitations with either the hydrogel formulation, the intensity of the electrical field or voltage applied, or the immersion solution being incompatible with mammalian cells. [89, 90] This investigation attempts to create an electroactive hydrogel that deforms in response to electrical stimulation and supports cells. The first step towards that goal must be the use of a cell-compatible hydrogel formulation.

2.4 PEG-based Electroactive Polymers

2.4.1 PEGDA

Poly(ethylene glycol) diacrylate (PEGDA) is a well-characterized polymer in tissue engineering. It is biocompatible, hydrophilic, resistant to protein absorption, non-immunogenic, and allows for diffusion of waste and nutrients. [91, 92] It is particularly favorable for examining cell response to materials mimicking the physical properties of soft tissues because it is mechanically tunable and lacks confounding biomechanical or

microarchitectural signals. PEG-based hydrogels owe their elastic properties to the inherently flexible chemical chain of PEG. [92-95] Cao et al. varied the concentration of PEGDA and gelatin and observed that these variations changed storage modulus and mesh size, which influenced the growth and morphology of neonatal human dermal fibroblasts. [92] Gunn et al. also varied PEGDA concentration in hydrogels and measured their Young's modulus and found a positive correlation to PEGDA concentration (Figure 2.2). [96] Neural cells seeded on hydrogels with a higher Young's modulus exhibited less neurite extension than those on lower modulus scaffolds. [96] Since PEGDA lacks biologically active sites and is resistant to protein absorption, it allows researchers to isolate the effects of mechanical properties on cells. Electroactive scaffolds have been constructed with polymers such as polycaprolactone (PCL) and polyaniline however there is limited research on PEG-based electroactive scaffolds. [97, 98] PEGDA provides a stable yet easily adjustable base for cell scaffold studies, particularly when examining how biophysical cues influence cells. Therefore, it is a promising candidate as the polymer base for electroactive hydrogels that will undergo mechanical deformation.

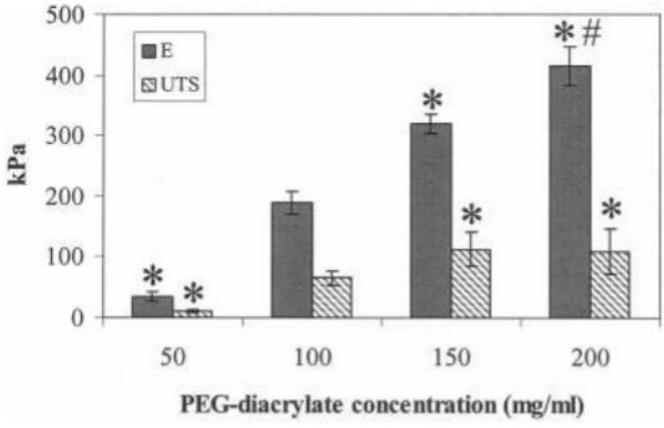

Figure 2.3 Relationship between PEGDA concentration and Young's Modulus. There is a positive correlation between Young's Modulus (E) and the concentration of PEGDA when used to formulate a scaffold. [96]

2.4.2 PAA in Tissue Scaffolds

Poly(acrylic acid) (PAA) is the product of the polymerization of acrylic acid, an organic compound that has applications in drug release and tissue engineering due to its biocompatibility, biodegradability, and mechanical stability. [99] Faturechi et al. created hydrogels with PAA (10-30 wt%) and subjected them to a series of compressive loads to determine their elastic modulus and maximum stress and strain. [99] They found that hydrogels at 30 wt% PAA exhibited a large decrease in Young's modulus but a significant increase in maximum strain. PAA also has a high molecular weight, which is valuable in hydrogels because it allows them to swell and retain water within their crosslinked network. [100, 101] Additionally, PAA is a suitable compound in pH responsive systems due to the presence of carboxylic acid side groups. PAA is a beneficial organic substance used in scaffold formation when cross-linked with a mechanically stable polymer.

2.4.3 PEGDA-PAA

PEGDA-PAA is a dynamic and suitable polymer combination for hydrogel products in tissue engineering due to the biocompatibility of both compounds as well as their individual properties of mechanical robustness and pH-responsive chemical structure. PEGDA-PAA hydrogels have shown potential in implant structures. [102] Farooqui et al. implanted a PEGDA-PAA hydrogel in the stroma of a bovine cornea to understand the scaffold's potential for cellular adhesion, tensile strength, and permeability to glucose. Results showed that PEGDA-PAA was 10 times stronger than PEGDA or PAA hydrogels alone and cell migration was greater on PEGDA-PAA hydrogels bound with collagen than those without collagen. [103] This suggests that cell adhesion ligands may be necessary when using PEGDA-PAA as a substrate. When polymerized, PEGDA-PAA forms a mesh-like, loosely crosslinked, ionizable network. [104] These characteristics cause the hydrogel to be mechanically tunable but also give it its electroactive nature. The hydrophobic acrylate groups in PEGDA and PAA cluster in an aqueous solution and are susceptible to free-radical polymerization. In the presence of photoinitators and a light source, both PEGDA and acrylic acid polymerize and covalently bind at the clustered acrylate groups. Crosslinks occur at the C=C sites and the ionic charges persist on the carboxylic acids when the hydrogens dissociate in the aqueous solution. When the polymerized hydrogel is exposed to an electric field, the ions within the hydrogel move towards the oppositely charged electrode and this mechanical movement of ions causes a conformational change in the polymer chains of the hydrogel causing it to bend in the direction the ions are moving (Figure 4.3). Despite their cytocompatibility and electroactive nature, PEGDA-PAA

hydrogels have not been explored for their potential as electroactive cell scaffolds – the work herein describes such an effort.

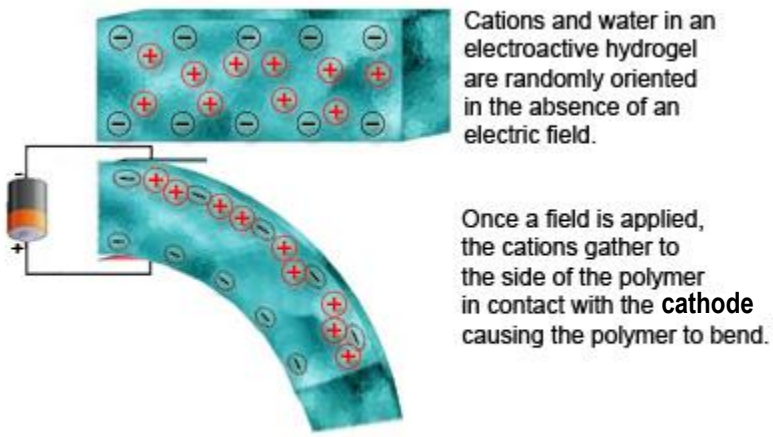

Figure 2.4 The movement of ions and water in an electroactive hydrogel in the absence and presence of an electric field.

CHAPTER 3. Materials and Methods

3.1. Hydrogel Preparation

Unless otherwise noted, all reagents used were obtained from Sigma Aldrich (St. Louis, MI, USA). All hydrogel formulations were created with 10 kDa PEGDA, 2,2-dimethoxy-2-phenylacetophenone (ACE), 1-vinyl-2-pyrrolidinone (NVP), 25 mM HEPES Buffered Saline (HBS), and acrylic acid (AA). A photo-initiator solution was prepared by fully dissolving ACE (300 mg) in NVP (1 mL). PEGDA (6.7% w/v), AA (3.3% v/v), and ACE-NVP (0.7% v/v) was fully dissolved in HBS and injected into a mold (2.5 cm × 1 cm × 0.5 mm) comprised of glass slides clamped together and separated by Teflon spacers. The mold was exposed to UV light (365 nm, 10 mW/cm^2) for 60 seconds. Polymerized hydrogels were removed from molds, washed in Dulbecco's phosphate-buffered saline (PBS), and held at 4 °C for 24 hours in either PBS or complete culture medium (Gibco Minimum Essential Media alpha (α-MEM) with nucleosides supplemented with 10% Gibco Fetal Bovine Serum and 1% Penicillin/Streptomycin).

3.2 Hydrogel Swelling Mass Characterization

After hydrogels were prepared (n=9), they were immediately weighed. Following weighing, the hydrogels were placed in either PBS or complete culture medium and allowed to swell for 24 hours at 4 °C. Following 4 hours of swelling, hydrogels were weighed a second time and the change in hydrogel swelling mass was calculated.

3.3. Electrical Stimulation of Hydrogels and Scaffolds

Hydrogels were cut to different aspect ratios. They were cut with a scalpel to a length of 13.62 ± 0.93 mm, 3.55 ± 0.46 mm, or 1.84 ± 0.09 mm with a consistent width of 4.58 mm ± 0.66 mm. Hydrogel actuation was conducted in 30% w/v NaCl solution, in complete culture medium, and in PBS. The cut hydrogels were placed in a polystyrene petri dish then immersed in one of the 3 solutions. Once hydrogels demonstrated movement in PBS and culture medium, the NaCl solution was not further examined. Platinum electrodes connected to an Agilent DC power supply (E3646A Agilent Technologies, Santa Clara, CA, USA) were placed in the immersion solution lengthwise on either side of the hydrogel without making direct contact with the hydrogels. The hydrogels were stimulated twice with a 1 min on/5 min off cycle at 20 V. A protractor was placed beneath petri dishes and hydrogels were imaged during stimulation to determine bending angles. The hydrogels were stained with food coloring by dispersing a drop of the colored liquid into the immersion solution prior to actuation.

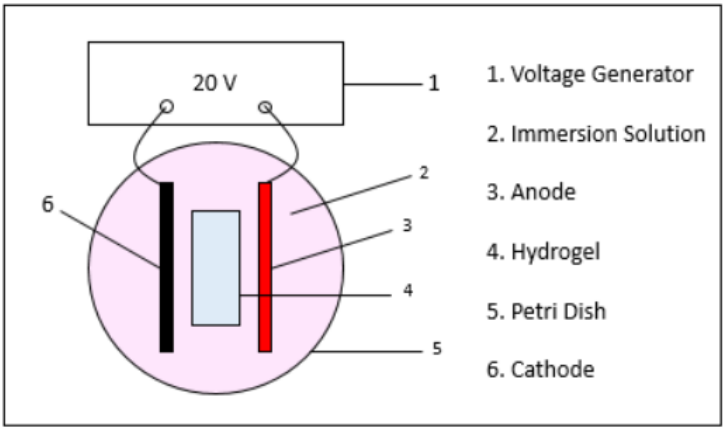

Figure 3.1 The electrical stimulation experimental setup. Platinum wires are used as the electrodes—an anode (black) and cathode (red) on either side of the hydrogel.

3.4. Biocompatibility of Hydrogels

3.4.1 Cell Culture

hMSCs were cultured with complete culture media and passaged every 2-3 days when cultures appeared 70-80% confluent. Cells were expanded until the total cell count exceeded 1.5 million cells. To harvest cells in preparation for encapsulation or seeding on a hydrogel, the cells were washed with PBS, trypsinized, diluted with complete culture media, spun in a centrifuge at 300g for 5 minutes, aspirated, and resuspended in complete culture media at $50x10^4$ cells/mL.

3.4.2 Cell Encapsulation

A 2X hydrogel solution and a cell suspension at 10^5 cells per mL was combined at a 1:1 volume ratio to create a hydrogel-cell prepolymer solution. The solution was injected into a mold then exposed to UV light (365 nm, 10 mW/cm^2) for 60 seconds. The polymerized,

cell-embedded hydrogels were immediately removed from the mold and immersed in cell media. The media was changed every 20 minutes for the first hour and every hour for the next 4 hours to wash the hydrogels of any excess un-polymerized PEGDA and AA. The cell-encapsulated hydrogels were kept immersed in cell media overnight in a humidified incubator with 5% CO_2 at 37°C. The media was changed once more before cells in the hydrogels were evaluated for viability at 24 hours.

3.4.3 PEG-RGDS Synthesis

Arg-Gly-Asp-Ser (RGDS) (Tocris) peptide was conjugated with acrylate-PEG-succinimidyl valerate (ACRL-PEG-SVA). A 1.2:1 ratio of RGDS (433 g/mol) to ACRL-PEG-SVA (3000 g/mol) (Laysan Bio, Arab, AL, USA) was used in the conjugation process. Lyophilized RGDS peptide was reconstituted in PBS (4 mL) in an amber vial. PEG-SVA was dissolved in PBS (2 mL) and dripped into the RGDS solution. The ACRL-PEG-RGDS solution was vortexed and titrated to pH 8.0 using 0.1 M sodium hydroxide. The vial was filled with argon, vortexed, and placed on an orbital shaker for 4 hours at the largest tilt and highest agitation settings. In the first 4 hours, the pH of the solution was checked every 45 minutes and readjusted to pH 8.0 if necessary. The vial was left on the shaker overnight to fully react. After 12-16 hours the solution was adjusted back to pH 7.0. The reaction was transferred to a 3500 molecular weight cutoff (MWCO) dialysis membrane which had been previously rinsed with Milli-Q water. The reaction was dialyzed against Milli-Q water (4 L), changing the water 4-5 times. The first two changes were made after 1 hour increments, the reaction was left overnight, and 2-3 more changes were made 1.5 hours apart the next day. The reaction was removed from the dialysis membraned and

frozen at -80°C for an hour. The frozen reagent was lyophilized for over 48 hours and stored under argon at -20°C until use.

3.4.4 Surface Conjugation

ACRL-PEG-RGDS (8 mg) was reconstituted in 0.5 mL of HEPES buffered saline (HBS) to form a stock solution. The stock solution (100 µL) was combined with HBS (200 µL), deionized water (DI) (200 µL), eosin Y (5 µL), and ACE/NVP photoinitiator solution (5 µL). This mixture was vortexed until fully combined. In preparation for surface conjugation, hydrogels were immersed in PBS or complete culture media at 4°C for 48 hours to allow swelling and washed with PBS (25 mL). The final RGDS solution (50 µL) was micro-pipetted onto one face of a hydrogel and exposed to collimated white light for 1 minute to photo-polymerize the RGDS onto the surface of the hydrogel. Hydrogels were placed in 6-well plates and over 48 hours were subjected to 5 exchanges of PBS and incubated in complete culture media in a humidified incubator at 37°C with 5.0% CO_2 to remove unbound RGDS.

3.4.5 Cell Seeding

hMSCs were harvested and resuspended at a 500,000 cells/mL concentration. The cell suspension (200 µL) was pipetted onto the RGDs-modified surface of hydrogels. Cell-seeded hydrogels were then immersed in media and placed in incubators. Complete cell media was changed every two days and viability studies were conducted on Days 1, 4, 7, 10, 14, and 22. Cell-seeded hydrogels were electrically stimulated on Day 4 as previously

described (section 3.2) with the following modifications: prepolymers were sterile-filtered and molds and instruments contacting hydrogels were disinfected with 70% ethanol.

3.4.6 Viability Assays

Hydrogels encapsulating cells and hydrogels with cells seeded on the surface were evaluated for viability 24 hours after cell encapsulation and on day 4 after cell seeding. Viability assays were performed using Ethidium homodimer-1/Calcein acetoxymethyl (AM) LIVE/DEAD® Viability/Cytotoxicity Kit (ThermoFisher, Waltham, MA, USA). Ethidium homodimer-1 is a nucleic acid stain that detects dead cells because it emits red fluorescence when bound to DNA, which is only accessible through the dead cells' permeable nuclei. Calcein AM converts to a green fluorescence when it undergoes hydrolysis in the presence of intracellular esterases and thus detects viable cells. Within a tissue culture hood, complete cell media was combined with ethidium homodimer-1 (0.2% v/v) and calcein AM (0.05% v/v), then vortexed. Hydrogels were placed in 6 well plates with 3 mL of the dye solution. Well plates were covered in aluminum foil and placed into incubators for 20 minutes before imaging. Hydrogels were washed with PBS (5 mL) to remove excess stain and then imaged under an epifluorescent microscope (Axio Observer ZI, Zeiss). Cells were observed at a 10x magnification with 2 fluorescent channels that labeled cells live (green, ex/em; ~450/475 nm) and dead (red, ex/em; ~600/635 nm). Three sets of images were captured for each hydrogel. Cross-sectional images for cell-encapsulated hydrogels were acquired using the Z-stack function in 20 nm increments through the thickness of the gel. 3D images were taken with the ApoTome at ~89 ms exposure time in the conventional fluorescence acquisition mode.

CHAPTER 4. Results

4.1. Hydrogel Swelling Characterization

Figure 4.1 depicts the average change in mass with respect to the immersion solution of the hydrogels immediately after synthesis. Changing the immersion solution from PBS to complete culture media increased the average change in mass by ~1.5 fold from 0.36 ± 0.053 grams to 0.52 ± 0.069 grams, $p= 5.56x10^{-5}$.

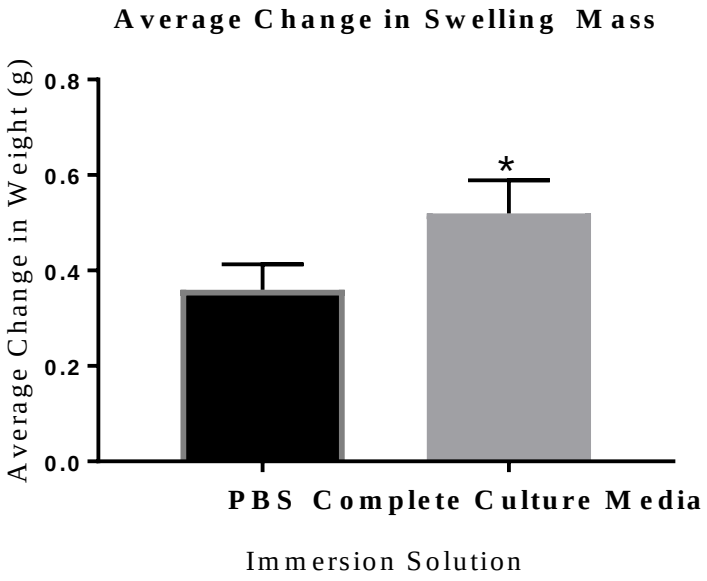

Figure 4.1 Hydrogel change in mass following swelling. Hydrogels were stored in PBS or complete culture media for 24 hours after generation. Their weights were measured before and after the 24 hour swelling period and the average change in mass was calculated (n=9). Error bars indicate standard deviation, asterisk indicates significant difference ($p< 0.05$).

4.2 Electrical Stimulation of Hydrogels

During the 1 minute of 20 V application, hydrogels experienced bending. The PEGDA-PAA hydrogels bent slowly and did not achieve full bending at the end of the minute. When stimulated for longer than one minute, the hydrogels continued to bend. Figure 4.3 shows graphs of average hydrogel bending angle with respect to aspect ratio of the hydrogel, immersion solution, and voltage. Reducing the aspect ratio by ~1/2 increased the bending angle by over 6 fold, from 8.25 ± 8.81 degrees to 52.8 ± 17.75 degrees, p = 0.004. Changing the immersion solution from PBS to complete culture media somewhat decreased the bending angle by 1.5 fold, from 36.25 ± 35.37 degrees to 24.75 ± 19.33, though the difference was not statistically significant. Doubling the stimulation voltage mildly increased the bending angle by 1.3 fold, from 26.50 ± 33.37 degrees to 34.50 ± 23.59 degrees, though the difference was not statistically significant.

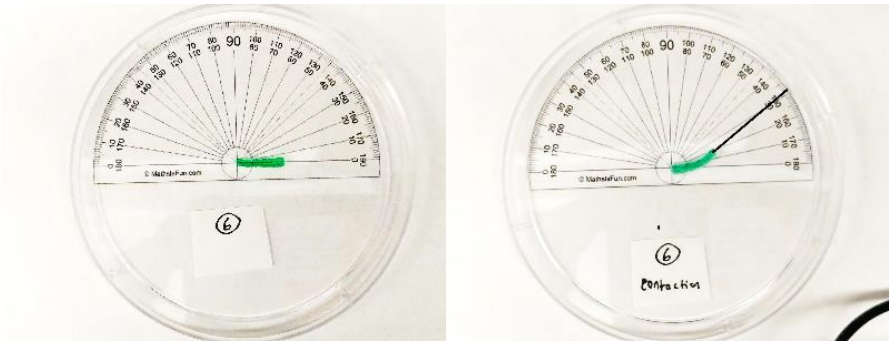

Figure 4.2 Electric stimulation of electroactive hydrogel. Electroactive hydrogel in relaxed (left) and stimulated (right) states. The clear hydrogel was stained prior to actuation to increase its visibility.

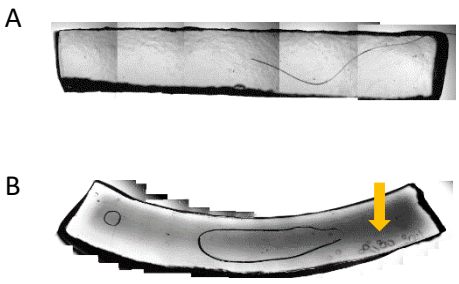

Figure 4.3 Photomerge of phase contrast images of hydrogel before (A) and after (B) stimulation. Arrow shows accumulation of bubbles on cathode side of gel. 5x magnification.

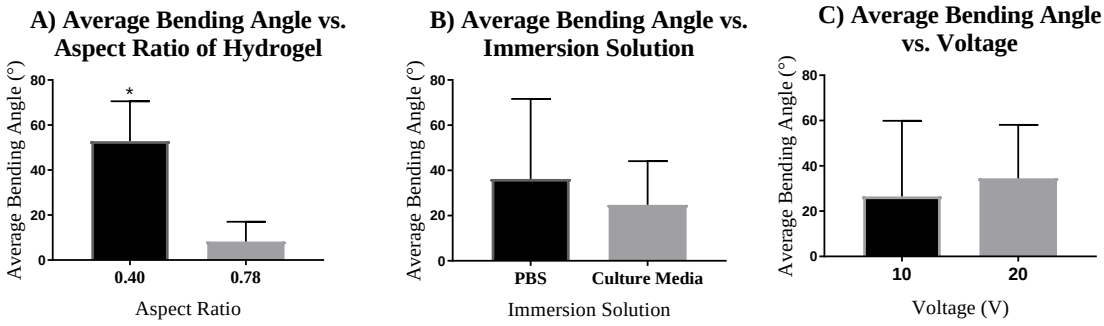

Figure 4.4 Amount of bending when varying actuation and hydrogel parameters. Column graphs compare bending angle of the PEG-PAA hydrogels during actuation when varying the A. aspect ratio of the hydrogel, B. immersion solution, and C. voltage. Four hydrogels were tested for each parameter. Error bars indicate standard deviation, asterisks indicate statistical significance ($p<0.05$).

4.2. Cell Viability Studies

4.2.1. Cell Encapsulation without Electrical Stimulation

To determine whether MSCs survive the encapsulation process, cell viability studies were conducted 24 hours after encapsulation. (Figure 4.4)

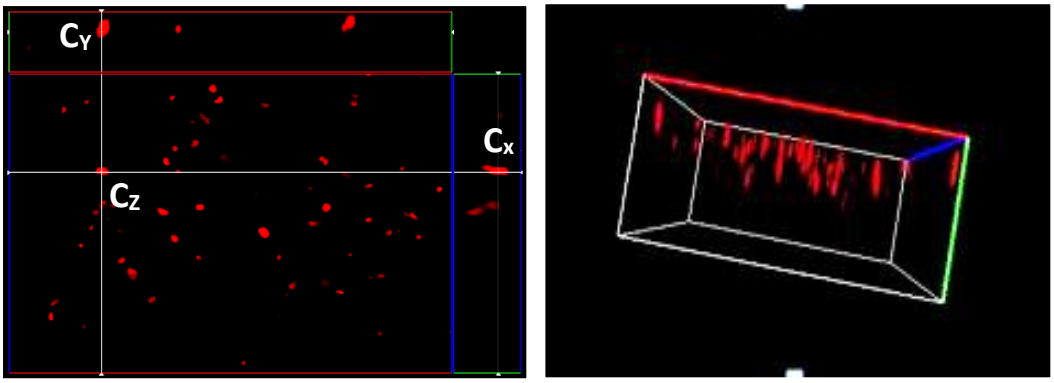

Figure 4.5 Stained images of cell-encapsulated hydrogel. Left: An image depicting x, y, and z views of the hydrogel after cell encapsulation. The red and blue lines indicate the margins of a z slice of the hydrogel. The area above the red line shows a y slice and the area to the right of the green line shows an x slice. The white cross-hatch shows a single cell as seen from the z plane (Cz), the y plane (C_Y), and the x plane (C_X) Right: An orthogonal z-stack projection of the hydrogel. The blue and red lines of each image correspond to each other. The red circular particles indicate dead cells and any green circular particles would indicate live cells. There was no cell viability post cell encapsulation.

4.2.2 Cell Seeding on Hydrogel Surfaces without Electrical Stimulation

A viability study was conducted on surface-seeded cells from day 1 until 22 days post seeding. (Figure 2) Throughout the 21 days, the cells proliferated and the percent viability

increased. Between days 1 and 14, the cells displayed a more circular morphology and were distinctly separated. By day 22, the cells had elongated and were clustered throughout the surface of the hydrogel showing evidence of migration and proliferation. Figure 4.5 graphs the percent viability for the 22 day culture.

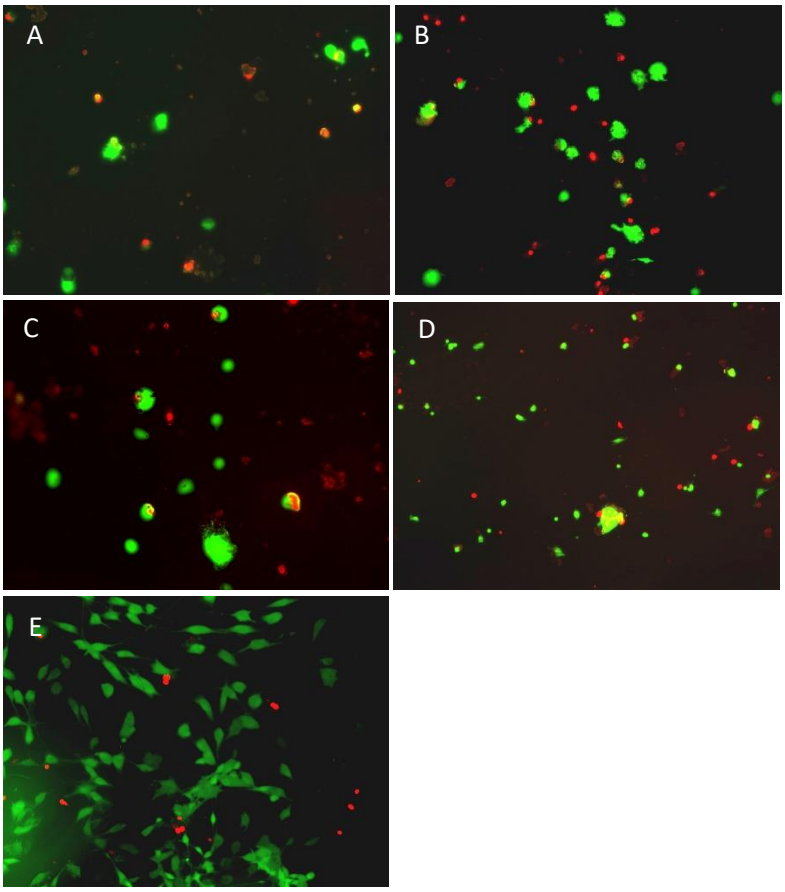

Figure 4.6 Ethidium homodimer 1 and calcien AM staining of hMSCs seeded on the surface of a PEG-PAA hydrogel for 22 days. Images are taken on A. Day 1, B. Day 3, C. Day 7, D. Day 14 and E. Day 22. Cells were observed at a 10x magnification with 2

fluorescent channels that labeled cells live (green, ex/em; ~450/475 nm) and dead (red, ex/em; ~600/635 nm).

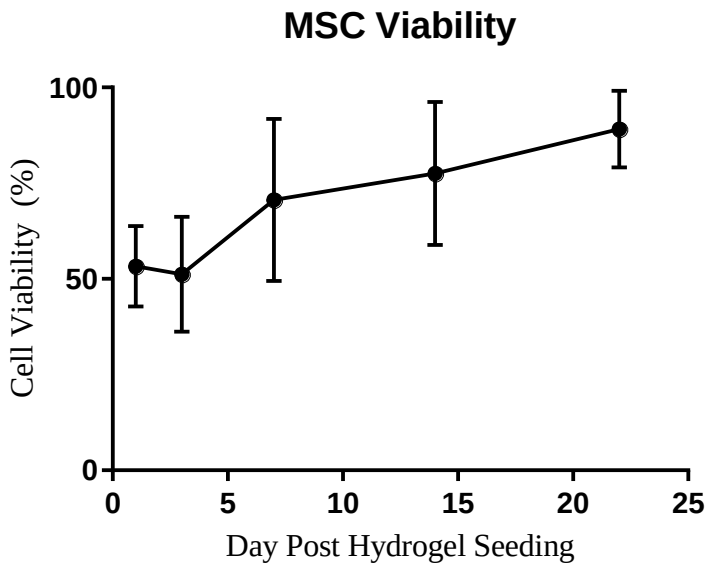

Figure 4.7 Percent cell viability of hMSCs seeded on a PEGDA-PAA hydrogels for 22 days. Error bars indicate standard deviation.

4.2.3. Electrical Stimulation of Hydrogels with Surface-Seeded Cells

Cell-seeded hydrogels were stimulated with 20 V in PBS or complete culture media and with 10 V with a DC power supply. All hydrogels prior to actuation had a flat and straight shape. After stimulation, the hydrogels exposed to 20 V displayed bending but the hydrogels exposed to 10 V did not. The deformation of the cell-seeded hydrogels was not altered by the presence of cells. Hydrogels actuated in PBS showed greater bending than those in complete culture medium. Viability studies determined that no hMSCs seeded on hydrogels survived the application of voltage at 10 or 20V. (Figure 4.7)

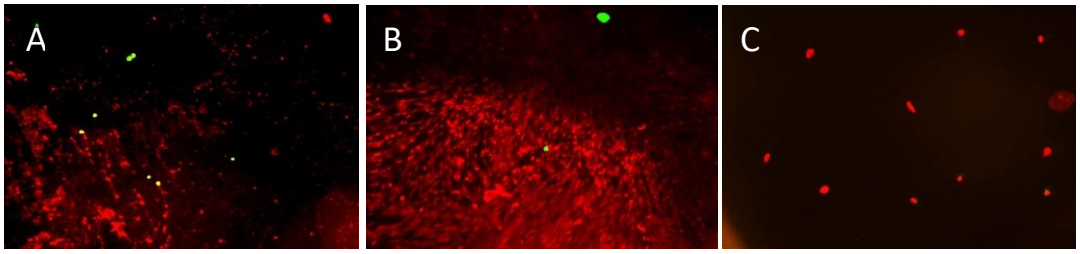

Figure 4.8 Stained images of cell-seeded hydrogels post actuation. Hydrogels were actuated at A. 20 V in PBS and B. 20 V in complete cell medium and at C. 10 V in PBS. All electrical stimulation was conducted for 60 seconds. Cells were observed at a 10x magnification with 2 fluorescent channels that labeled cells live (green, ex/em; ~450/475 nm) and dead (red, ex/em; ~600/635 nm). All 3 conditions showed zero viability post voltage stimulation.

CHAPTER 5. Discussion

This investigation evaluated PEGDA-PAA hydrogels towards their development as cell scaffolds. A long term goal is to use these scaffolds to expose MSCs to mechanical stresses and observe their resulting behavior. The hydrogel discussed in this study is the only PEGDA-PAA hydrogel that is both capable of supporting cells and responds by bending when exposed to electric stimuli. The studies discussed have provided evidence that this hydrogel responds to electric currents when submersed in cell viable solutions, a step forward from previous electroactive scaffold studies that use a concentrated sodium chloride solution that would not be feasible for cell application. [105] When varying voltage, hydrogel aspect ratio, and immersion solution during electrical stimulation of the hydrogels, the degree of hydrogel bending was most impacted by change in hydrogel aspect ratio (p=0.004). A thinner hydrogel resulted in a larger bending angle during electrical stimulation. From beam theory, this puts the concave side of the beam in compression and the convex side in tension. Therefore, hydrogel aspect ratio can be used as a variable to subject seeded cells to strains ranging from compressive to tensile. Kim et al. showed greater bending of their electroactive hydrogels at higher voltages. [105, 106] In this study, although a larger voltage also increased bending angle, it was not significant (p=0.709).

Cell viability was examined following encapsulation and surface seeding. Encapsulated cells did not survive hydrogel formulation. This is likely due to the high concentration of acrylic acid exposure. [107] UV light has been used to encapsulate cells, therefore it is unlikely that such exposure caused the lack of cell viability. Sabnis et al. used UV light (365 nm, 10 mW/cm^2) for 1-5 minutes to encapsulate cells in poly(*N*-isopropylacrylamide)-PEGDA hydrogels and showed that cells in hydrogels exposed to

different lengths of UV light had the same relative survival as cells in hydrogels formed in the absence of UV light. [108] Although the encapsulation in this study was lethal to cells, as a substrate the results were promising. In the initial days, cells were balled on the surface of the hydrogels. This could be due to incomplete rinsing of unbound PEG-RGDS. It has been demonstrated that when RGDS is in solution, it inhibits cell adhesion. [109] In future studies, the surface chemistry of these hydrogels could be examined using fourier transformed infrared spectroscopy. [110] By Day 22, cells had multiplied and over 85% of the cells were viable and were spread over the surface of the hydrogel. The conjugation of RGDS peptide to the surface of the PEGDA-PAA hydrogels did not interfere with the bending of the hydrogel during actuation.

Electrical stimulation of cell-seeded hydrogels resulted in complete cell death. This is most likely due to the large current the cells experienced when stimulated. Other investigations that incorporated cells into electroconductive hydrogels have shown that their cells survive when using voltages ranging from 50-640 mV. [78, 79, 111] The work presented herein used orders of magnitude greater, at 10 and 20 V. Unfortunately, however when dose response actuation studies were performed, the PEGDA-PAA hydrogel did not exhibit bending behavior with voltages below 10 V. Thus, there is a trade-off between cell viability and hydrogel movement. This may explain why the bulk of research examining electroactive materials do not explore the incorporation of cells. [106, 112-115]

CHAPTER 6. Conclusions and Future Directions

This investigation evaluated an electroactive hydrogel for its ability to deform, the degree of deformation, at various actuation parameters as well as the cytocompatibility of the hydrogel before and after stimulation. The PEGDA-PAA hydrogel exhibited reversible contractile behavior when exposed to voltages at 10 and 20 volts. The hydrogel was not compatible with hMSCs when they were encapsulated within its 3D structure but proved a suitable substrate when these cells were seeded on the surface of the hydrogel with the integrin adhesion peptide RGDS. When hydrogels seeded with hMSCs were stimulated at 10 and 20 volts, cells were killed and were washed off the hydrogel. Continued efforts in this study will focus on reducing the voltage delivered to the hydrogel while optimizing its bending. This may be performed by using a square wave that has discrete peaks of higher voltage but a lower average voltage. Another alternative method could position the electrodes to make direct contact with the hydrogel in an area where there are no cells. This could allow the use of a lower voltage with the same degree of bending.

Finally, the stiffness of the hydrogel could be examined and potentially reduced with a higher molecular weight PEGDA. Mazzoccoli et al. studied mechanical properties with low and high molecular weight PEGDA scaffolds. [116] The results showed that compliance increased with the incorporation of higher molecular weight PEGDA. These findings may be translatable to the PEGDA-PAA polymer and increasing PEGDA molecular weight may increase hydrogel flexibility, which in turn may allow bending to a similar degree but with a smaller voltage.

If cell viability can be achieved while electrically actuating these hydrogels, further studies to explore how these actuating hydrogels might affect the differentiation of MSCs could be conducted. Electrical stimulation could then be harnessed to possibly even control MSC differentiation and enhance the PEGDA-PAA hydrogel's ability to serve as a cell scaffold that resembles excitable tissues.

References

1. Haj, J., et al., *An ECM-Mimicking, Mesenchymal Stem Cell-Embedded Hybrid Scaffold for Bone Regeneration.* Biomed Res Int, 2017. **2017**: p. 8591073.
2. Shimomura, K., B.B. Rothrauff, and R.S. Tuan, *Region-Specific Effect of the Decellularized Meniscus Extracellular Matrix on Mesenchymal Stem Cell-Based Meniscus Tissue Engineering.* Am J Sports Med, 2017. **45**(3): p. 604-611.
3. Urnukhsaikhan, E., et al., *Pulsed electromagnetic fields promote survival and neuronal differentiation of human BM-MSCs.* Life Sci, 2016. **151**: p. 130-138.
4. Zhao, L., et al., *Effects of IGF-1 on neural differentiation of human umbilical cord derived mesenchymal stem cells.* Life Sci, 2016. **151**: p. 93-101.
5. Horner, C.B., et al., *Microstructure-dependent mechanical properties of electrospun core-shell scaffolds at multi-scale levels.* J Mech Behav Biomed Mater, 2016. **59**: p. 207-219.
6. Kelly, D.J. and C.R. Jacobs, *The role of mechanical signals in regulating chondrogenesis and osteogenesis of mesenchymal stem cells.* Birth Defects Res C Embryo Today, 2010. **90**(1): p. 75-85.
7. Huang, C.Y., et al., *Effects of cyclic compressive loading on chondrogenesis of rabbit bone-marrow derived mesenchymal stem cells.* Stem Cells, 2004. **22**(3): p. 313-23.
8. Campbell, J.J., D.A. Lee, and D.L. Bader, *Dynamic compressive strain influences chondrogenic gene expression in human mesenchymal stem cells.* Biorheology, 2006. **43**(3,4): p. 455-70.
9. Moffat, K.L., et al., *Composite Cellularized Structures Created from an Interpenetrating Polymer Network Hydrogel Reinforced by a 3D Woven Scaffold.* Macromol Biosci, 2018: p. e1800140.
10. Pelaez, D., C.Y. Huang, and H.S. Cheung, *Cyclic compression maintains viability and induces chondrogenesis of human mesenchymal stem cells in fibrin gel scaffolds.* Stem Cells Dev, 2009. **18**(1): p. 93-102.
11. Tzeng, W.R., et al., *Treatment of osteoarthritis with collagen-based scaffold: A porcine animal model with xenograft mesenchymal stem cells.* Histol Histopathol, 2018: p. 18013.
12. Pelaez, D., C.Y. Huang, and H.S. Cheung, *Cyclic compression maintains viability and induces chondrogenesis of human mesenchymal stem cells in fibrin gel scaffolds.* Stem Cells Dev, 2009. **18**(1): p. 93-102.
13. Charoenpanich, A., et al., *Cyclic tensile strain enhances osteogenesis and angiogenesis in mesenchymal stem cells from osteoporotic donors.* Tissue Eng Part A, 2014. **20**(1-2): p. 67-78.
14. Ghazanfari, S., M. Tafazzoli-Shadpour, and M.A. Shokrgozar, *Effects of cyclic stretch on proliferation of mesenchymal stem cells and their differentiation to smooth muscle cells.* Biochem Biophys Res Commun, 2009. **388**(3): p. 601-5.
15. Song, G., et al., *Mechanical stretch-induced changes in cell morphology and mRNA expression of tendon/ligament-associated genes in rat bone-marrow mesenchymal stem cells.* Mol Cell Biomech, 2010. **7**(3): p. 165-74.

16. Burk, J., et al., *Induction of Tenogenic Differentiation Mediated by Extracellular Tendon Matrix and Short-Term Cyclic Stretching.* Stem Cells Int, 2016. **2016**: p. 7342379.
17. Kim, H.J. and J.S. Park, *Usage of Human Mesenchymal Stem Cells in Cell-based Therapy: Advantages and Disadvantages.* Dev Reprod, 2017. **21**(1): p. 1-10.
18. Trento, C., et al., *Manufacturing Mesenchymal Stromal Cells for the Treatment of Graft-versus-Host Disease: A Survey among Centers Affiliated with the European Society for Blood and Marrow Transplantation.* Biol Blood Marrow Transplant, 2018.
19. Heo, S.J., et al., *Differentiation alters stem cell nuclear architecture, mechanics, and mechano-sensitivity.* Elife, 2016. **5**.
20. Huang, C., J. Dai, and X.A. Zhang, *Environmental physical cues determine the lineage specification of mesenchymal stem cells.* Biochim Biophys Acta, 2015. **1850**(6): p. 1261-6.
21. Meyer, M.B., et al., *Epigenetic Plasticity Drives Adipogenic and Osteogenic Differentiation of Marrow-derived Mesenchymal Stem Cells.* J Biol Chem, 2016. **291**(34): p. 17829-47.
22. Lee, M.S., et al., *Endothelin-1 differentially directs lineage specification of adipose- and bone marrow-derived mesenchymal stem cells.* FASEB J, 2018: p. fj201800614R.
23. Fazzi, R., et al., *Mesodermal progenitor cells (MPCs) differentiate into mesenchymal stromal cells (MSCs) by activation of Wnt5/calmodulin signalling pathway.* PLoS One, 2011. **6**(9): p. e25600.
24. Huang, A.H., et al., *Long-term dynamic loading improves the mechanical properties of chondrogenic mesenchymal stem cell-laden hydrogel.* Eur Cell Mater, 2010. **19**: p. 72-85.
25. Wang, W., et al., *Elongated cell morphology and uniaxial mechanical stretch contribute to physical attributes of niche environment for MSC tenogenic differentiation.* Cell Biol Int, 2013. **37**(7): p. 755-60.
26. Tan, A.R., et al., *Passage-dependent relationship between mesenchymal stem cell mobilization and chondrogenic potential.* Osteoarthritis Cartilage, 2015. **23**(2): p. 319-27.
27. Izadpanah, R., et al., *Long-term in vitro expansion alters the biology of adult mesenchymal stem cells.* Cancer Res, 2008. **68**(11): p. 4229-38.
28. Heo, S.J., et al., *Expansion of mesenchymal stem cells on electrospun scaffolds maintains stemness, mechano-responsivity, and differentiation potential.* J Orthop Res, 2018. **36**(2): p. 808-815.
29. Rashedi, I., et al., *Collagen scaffold enhances the regenerative properties of mesenchymal stromal cells.* PLoS One, 2017. **12**(10): p. e0187348.
30. Urciuolo, A. and P. De Coppi, *Decellularized Tissue for Muscle Regeneration.* Int J Mol Sci, 2018. **19**(8).
31. El-Jawhari, J.J., et al., *Collagen-containing scaffolds enhance attachment and proliferation of non-cultured bone marrow multipotential stromal cells.* J Orthop Res, 2016. **34**(4): p. 597-606.

32. Intini, C., et al., *3D-printed chitosan-based scaffolds: An in vitro study of human skin cell growth and an in-vivo wound healing evaluation in experimental diabetes in rats.* Carbohydr Polym, 2018. **199**: p. 593-602.
33. Sancilio, S., et al., *Alginate/Hydroxyapatite-Based Nanocomposite Scaffolds for Bone Tissue Engineering Improve Dental Pulp Biomineralization and Differentiation.* Stem Cells Int, 2018. **2018**: p. 9643721.
34. McAndrews, K.M., et al., *Architectural and mechanical cues direct mesenchymal stem cell interactions with crosslinked gelatin scaffolds.* Tissue Eng Part A, 2014. **20**(23-24): p. 3252-60.
35. Yang, Q., et al., *A cartilage ECM-derived 3-D porous acellular matrix scaffold for in vivo cartilage tissue engineering with PKH26-labeled chondrogenic bone marrow-derived mesenchymal stem cells.* Biomaterials, 2008. **29**(15): p. 2378-87.
36. Gilbert, T.W., T.L. Sellaro, and S.F. Badylak, *Decellularization of tissues and organs.* Biomaterials, 2006. **27**(19): p. 3675-83.
37. Del Gaudio, C., et al., *Are synthetic scaffolds suitable for the development of clinical tissue-engineered tubular organs?* J Biomed Mater Res A, 2014. **102**(7): p. 2427-47.
38. Pok, S., *Design of synthetic scaffolds for tissue regeneration applications.* ProQuest, 2010.
39. Fallahiarezoudar, E., et al., *A review of: application of synthetic scaffold in tissue engineering heart valves.* Mater Sci Eng C Mater Biol Appl, 2015. **48**: p. 556-65.
40. Zhuravleva, M., et al., *In vitro assessment of electrospun polyamide-6 scaffolds for esophageal tissue engineering.* J Biomed Mater Res B Appl Biomater, 2018.
41. Kim, H.-J., J.-H. Lee, and G.-i. Im, *Chondrogenesis using mesenchymal stem cells and PCL scaffolds.* Biomedical Materails Research Part A, 2009. **92A**(2).
42. Haghighipour, N., et al., *Differential effects of cyclic uniaxial stretch on human mesenchymal stem cell into skeletal muscle cell.* Cell Biol Int, 2012. **36**(7): p. 669-75.
43. Leong, W.S., et al., *Cyclic tensile loading regulates human mesenchymal stem cell differentiation into neuron-like phenotype.* J Tissue Eng Regen Med, 2012. **6 Suppl 3**: p. s68-79.
44. Webber, M.J., et al., *A perspective on the clinical translation of scaffolds for tissue engineering.* Ann Biomed Eng, 2015. **43**(3): p. 641-56.
45. Armstrong, C., *Some General Properties of Excitable Tissues.* Physiology of Membrane Disorders, 1978.
46. Tandon, N., et al., *Electrical stimulation systems for cardiac tissue engineering.* Nat Protoc, 2009. **4**(2): p. 155-73.
47. Radisic, M., et al., *Functional assembly of engineered myocardium by electrical stimulation of cardiac myocytes cultured on scaffolds.* Proc Natl Acad Sci U S A, 2004. **101**(52): p. 18129-34.
48. Radisic, M., et al., *Biomimetic approach to cardiac tissue engineering.* Philos Trans R Soc Lond B Biol Sci, 2007. **362**(1484): p. 1357-68.
49. Ito, A., et al., *Induction of functional tissue-engineered skeletal muscle constructs by defined electrical stimulation.* Sci Rep, 2014. **4**: p. 4781.

50. Ross, J.J., M.J. Duxson, and A.J. Harris, *Neural determination of muscle fibre numbers in embryonic rat lumbrical muscles.* Development, 1987. **100**(3): p. 395-409.
51. Chi, N. and R. Wang, *Electrospun protein-CNT composite fibers and the application in fibroblast stimulation.* Biochem Biophys Res Commun, 2018.
52. Golafshan, N., M. Kharaziha, and M. Alehosseini, *A three-layered hollow tubular scaffold as an enhancement of nerve regeneration potential.* Biomed Mater, 2018. **13**(6): p. 065005.
53. Yuan, X., et al., *Electrical stimulation enhances cell migration and integrative repair in the meniscus.* Sci Rep, 2014. **4**: p. 3674.
54. *Chapter 13 - Cardiac Function*. Physiology 101 2011 2011; Available from: http://droualb.faculty.mjc.edu/Course%20Materials/Physiology%20101/Chapter%20Notes/Fall%202011/chapter_13%20Fall%202011.htm.
55. Ning, C., et al., *Electroactive polymers for tissue regeneration: Developments and perspectives.* Prog Polym Sci, 2018. **81**: p. 144-162.
56. Punning, A., et al., *Ionic electroactive polymer artificial muscles in space applications.* Sci Rep, 2014. **4**: p. 6913.
57. Bar-cohen, Y., *Electroactive Polyerms as Artificial Msucles- Reality and Challenges.* American Institute of Aeronautics and Astronautics, 2001.
58. Hunter, I.W. and S. Lafontaine, *A comparison of muscle with artificil actuators.* Technical Digest IEEE Solid-State Sensor and Actuator Workshop, 1992: p. 178-185.
59. Smela, E., *Conjugated Polymer Actuators for Biomedical Applications.* Adv. Mater., 2003. **15**(6): p. 481-494.
60. Vincenzini, P., *Artificial Muscle Actuators Using Electroactive Polymers*. 1 ed. Advances in Science and Technology, ed. Y. Bar-Cohen, F. Carpi, and P. Vincenzini. Vol. 61. 2008: Trans Tech Publications, Limited.
61. Alici, G., et al., *Response Characterization of Electroactive Polymers as Mechanical Sensors.* IEEE/ASME TRANSACTIONS ON MECHATRONICS, 2008. **13**(2): p. 187-196.
62. Baughman, R.H., *Conducting polymer artificial muscles.* Synthetic Metals, 1996. **78**(3): p. 339-353.
63. Wu, Y., et al., *Fast trilayer polypyrrole bending actuators for high speed applications.* Synthetic Metals, 2006. **156**(16-17): p. 1017-1022.
64. Bar-Cohen, Y., *Electroactive Polymers as Actuators*. 2 ed. Advanced Piezoelectric Materials. 2017: Woohead Publishing in Materials. 319-352.
65. Jones, R.W., *Artificial Muscles: Dielectric Electroactive Polymer-Based Actuation.* 2009 Second International Conference on Computer and Electrical Engineering, 2009: p. 209-216.
66. Pezzin, L.E., et al., *Use and satisfaction with prosthetic limb devices and related services.* Arch Phys Med Rehabil, 2004. **85**(5): p. 723-729.
67. Bundhoo, V. and E.J. Park, *Design of an artificial muscle actuated finger towards biomimetic prosthetic hands.* 12th International Conference on Advanced Robotics, 2005: p. 368-375.
68. Kim, K.J., et al., *Biomimetic Robotic Artificial Muscles*. 2013.

69. Mahdavian, M., A. Mahdavian, and A. Yousefi-Koma, *Design and Fabrication of a Robotic Hand Using Shape Memory Alloy Actuators.* 2015.
70. Kwon, G.H., et al., *Biomimetic soft multifunctional miniature aquabots.* Small, 2008. **4**(12): p. 2148-53.
71. Jager, E.W., O. Inganas, and I. Lundstrom, *Microrobots for micrometer-size objects in aqueous media: potential tools for single-cell manipulation.* Science, 2000. **288**(5475): p. 2335-8.
72. Balint, R., N.J. Cassidy, and S.H. Cartmell, *Conductive polymers: towards a smart biomaterial for tissue engineering.* Acta Biomater, 2014. **10**(6): p. 2341-53.
73. Zarrintaj, P., et al., *A Novel Electroactive Agarose-Aniline Pentamer Platform as a Potential Candidate for Neural Tissue Engineering.* Scientific Reports, 2017. **7**(1): p. 17187.
74. Hardy, J.G., et al., *Electroactive Tissue Scaffolds with Aligned Pores as Instructive Platforms for Biomimetic Tissue Engineering.* Bioengineering, 2015. **2**(1): p. 15-34.
75. Li, M.-y., et al., *Electroactive and nanostructured polymers as scaffold materials for neuonal and cardiac tissue engineering.* Chinese Journal of Polymer Science, 2007. **25**(04).
76. Rutten, W.L., *Selective electrical interfaces with the nervous system.* Annu Rev Biomed Eng, 2002. **4**: p. 407-52.
77. Thompson, D.M., et al., *Electrical stimuli in the central nervous system microenvironment.* Annu Rev Biomed Eng, 2014. **16**: p. 397-430.
78. Mawad, D., et al., *A Single Component Conducting Polymer Hydrogel as a Scaffold for Tissue Engineering.* Advanced Functional Materials, 2012. **22**: p. 2692-2699.
79. Liu, Y., et al., *Synthesis and characterization of novel biodegradable and electroactive hydrogel based on aniline oligomer and gelatin.* Macromol Biosci, 2012. **12**(2): p. 241-50.
80. Hahn, M.S., J.S. Miller, and J.L. West, *Three-Dimensional Biochemical and Biomechanical Patterning of Hydrogels for Guiding Cell Behavior.* Advanced Materials, 2006. **18**(20): p. 2679-2684.
81. Gelmi, A., et al., *Electroactive 3D Materials for Cardiac Tissue Engineering.* Electroactive Polymer Actuators and Devices, 2015. **9430**.
82. Li, Y., et al., *Electroactive BaTiO3 nanoparticle-functionalized fibrous scaffolds enhance osteogenic differentiation of mesenchymal stem cells.* Int J Nanomedicine, 2017. **12**: p. 4007-4018.
83. Balint, R., N.J. Cassidy, and S.H. Cartmell, *Electrical stimulation: a novel tool for tissue engineering.* Tissue Eng Part B Rev, 2013. **19**(1): p. 48-57.
84. Brighton, C.T., et al., *Signal transduction in electrically stimulated bone cells.* J Bone Joint Surg Am, 2001. **83-A**(10): p. 1514-23.
85. Huo, R., et al., *Noninvasive electromagnetic fields on keratinocyte growth and migration.* J Surg Res, 2010. **162**(2): p. 299-307.
86. Mendonca, A.C., C.H. Barbieri, and N. Mazzer, *Directly applied low intensity direct electric current enhances peripheral nerve regeneration in rats.* J Neurosci Methods, 2003. **129**(2): p. 183-90.

87. Li, Y., et al., *Electric Field Actuation of Tough Electroactive Hydrogels Cross-Linked by Functional Triblock Copolymer Micelles.* ACS Appl Mater Interfaces, 2016. **8**(39): p. 26326-26331.
88. Kwon, I.C., Y.H. Bae, and S. Kim, *Characteristics of Charged Networks Under an Electric Stimulus.* Journal of Polymer Science Part B: Polymer Physics, 1994. **32**: p. 1083-1092.
89. Yang, C., et al., *Hydrogel Walkers with Electro-Driven Motility for Cargo Transport.* Sci Rep, 2015. **5**: p. 13622.
90. Morales, D., et al., *Electro-actuated hydrogel walkers with dual responsive legs.* Soft Matter, 2014. **10**(9): p. 1337-48.
91. Zhu, J., *Bioactive modification of poly(ethylene glycol) hydrogels for tissue engineering.* Biomaterials, 2010. **31**(17): p. 4639-56.
92. Cao, Y., et al., *Synthesis of stiffness-tunable and cell-responsive Gelatin-poly(ethylene glycol) hydrogel for three-dimensional cell encapsulation.* J Biomed Mater Res A, 2016. **104**(10): p. 2401-11.
93. Jamadi, M., et al., *Poly (Ethylene Glycol)-Based Hydrogels as Self-Inflating Tissue Expanders with Tunable Mechanical and Swelling Properties.* Macromol Biosci, 2017. **17**(8).
94. Im, S.J., et al., *Synthesis and characterization of biodegradable elastic hydrogels based on poly(ethylene glycol) and poly(ε-caprolactone) blocks.* Macromolecular Research, 2007. **15**(4): p. 363-369.
95. Ravi, P., et al., *Three-dimensional printing of poly(glycerol sebacate fumarate) gadodiamide-poly(ethylene glycol) diacrylate structures and characterization of mechanical properties for soft tissue applications.* J Biomed Mater Res B Appl Biomater, 2018.
96. Gunn, J.W., S.D. Turner, and B.K. Mann, *Adhesive and mechanical properties of hydrogels influence neurite extension.* J Biomed Mater Res A, 2005. **72**(1): p. 91-7.
97. Hardy, J.G., et al., *Electroactive Tissue Scaffolds with Aligned Pores as Instructive Platforms for Biomimetic Tissue Engineering.* Bioengineering (Basel), 2015. **2**(1): p. 15-34.
98. Wu, Y., et al., *Fabrication of conductive polyaniline hydrogel using porogen leaching and projection microstereolithography.* Journal of Materials Chemistry B, 2015. **3**(26): p. 2352-2360.
99. Faturechi, R., et al., *Influence of Poly(arylic acid) on the Mechanical Properties of Composite Hydrogels.* Advances in Polymer Technology, 2014.
100. Jiang, Z., X. Cao, and L. Guo, *Synthesis and swelling behavior of poly (acrylic acid-acryl amide-2-acrylamido-2-methyl-propansulfonic acid) superabsorbent copolymer.* Journal of Petroleum Exploration and Production Technology, 2017. **7**(1): p. 69-75.
101. Hong, T.T. and K. Hara, *Radiation synthesis and characterization of super-absorbing hydrogel from natural polymers and vinyl monomer.* Environmental Polluiton, 2018. **242**: p. 1458-1466.
102. Zhou, C., et al., *Synthesis and characterization of well-defined PAA–PEG multi-responsive hydrogels by ATRP and click chemistry.* RSC Advances, 2014. **4**(97): p. 54631-54640.

103. Farooqui, N., et al., *Histological Evaluation of Poly(Ethylene Glycol)–Poly(Acrylic Acid) (PEG–PAA) Double Network Hydrogel Corneal Implant.* Investigative Ophthalmology & Visual Science, 2005. **46**(13): p. 873-873.
104. Zheng, L.L., et al., *Biocompatibility of poly(ethylene glycol) and poly(acrylic acid) interpenetrating network hydrogel by intrastromal implantation in rabbit cornea.* J Biomed Mater Res A, 2015. **103**(10): p. 3157-65.
105. Kim, S.J., et al., *Behavior in electric fields of smart hydrogels with potential application as bio-inspired actuators.* Smart Materials and Structures, 2005. **14**(4).
106. Kim, S.J., et al., *Bending behavior of hydrogels composed of poly(methacrylic acid) and alginate by electrical stimulus.* Polymer International, 2004. **53**: p. 1456-1460.
107. Yoshii, E., *Cytotoxic effects of acrylates and methacrylates: relationships of monomer structures and cytotoxicity.* J Biomed Mater Res, 1997. **37**(4): p. 517-24.
108. Sabnis, A., et al., *Cytocompatibility studies of an in situ photopolymerized thermoresponsive hydrogel nanoparticle system using human aortic smooth muscle cells.* J Biomed Mater Res A, 2009. **91**(1): p. 52-9.
109. Wu, P., et al., *Integrin-binding peptide in solution inhibits or enhances endothelial cell migration, predictably from cell adhesion.* Ann Biomed Eng, 1994. **22**(2): p. 144-52.
110. Browe, D.P., et al., *Characterization and optimization of actuating poly(ethylene glycol) diacrylate/acrylic acid hydrogels as artificial muscles.* Polymer, 2017. **117**: p. 331-341.
111. Yeo, W.S., M.N. Yousaf, and M. Mrksich, *Dynamic interfaces between cells and surfaces: electroactive substrates that sequentially release and attach cells.* J Am Chem Soc, 2003. **125**(49): p. 14994-5.
112. Moschou, E.A., et al., *Voltage-switchable Artificial Muscles Actuating at Near Neutral pH.* Sensors and Actuators B: Chemical, 2006. **115**(1): p. 379-383.
113. O'Grady, M.L., P.-l. Kuo, and K.K. Parker, *Optimization of Electroactive Hydrogel Actuators.* Applied Materials & Interfaces, 2009. **2**(2): p. 343-346.
114. Onoda, M., et al., *Artificial Muscle Using Conducting Polymers.* Denki Gakkai Ronbunshi, 2004. **124-A**(2): p. 120-125.
115. Yao, L. and S. Krause, *Electromechanical Responses of Strong Acid Polymer Gels in DC Electric Fields.* Macromolecules, 2003. **36**(6): p. 2055-2065.
116. Mazzoccoli, J.P., et al., *Mechanical and cell viability properties of crosslinked low- and high-molecular weight poly(ethylene glycol) diacrylate blends.* J Biomed Mater Res A, 2010. **93**(2): p. 558-66.